DOI 10.1007/s11182-017-1152-1

Russian Physics Journal, Vol. 60, No. 5, September, 2017 (Russian Original No. 5, May, 2017)

AN ELECTRON-MICROSCOPY ANALYSIS OF THE GRADIENT STRUCTURE FORMED IN TITANIUM DURING DEPOSITION OF A HARD COATING

Yu. F. Ivanov,[1,2,3] V. V. Shugurov,[1,3] O. V. Krysina,[1,2] E. A. Petrikova,[1,2] O. V. Ivanova,[4] and O. S. Tolkachev[3]

UDC 533.9: 539.4.015.2

A titanium nitride coating 0.5 μm in thickness is deposited on specimens of VT1-0 technical-grade titanium using a vacuum-arc, plasma-assisted process. The formation of a multilayer, multiphase highly defective structure is observed, whose thickness reaches up to 40 μm. Surface and transition layers are determined from the morphological characteristics. It is shown that the surface layer (300–350 nm thick), where the major phase is TiN*, possesses polycrystalline structure (crystallite size is 20–50 nm). The transition layer, whose major phase is* Ti_2N*, is divided into two sublayers. The sublayer immediately adjacent to the surface layer has columnar structure (transverse cross section of the columns is 50–80 nm). The sublayer bordering the bulk of the specimen is formed by quasi-equiaxed crystallites (150–280 nm). The main reason for formation of the multilayer, multiphase structure is thought to be the multistage character of material modification under conditions of common vacuum.*

Keywords: technically pure titanium, hard nitride coating, multilayer gradient structure, phase composition, properties.

INTRODUCTION

The main disadvantage of titanium and its alloys is their low wear resistance, which significantly limits the range of their industrial applications [1]. One of the ways of improving wear resistance of metals, including titanium and alloys frequently used in Russia and other countries, is deposition of high-hardness, wear-resistant coatings of various elemental compositions [2]. At present, functionally thin (1–5 μm) coatings are formed by such PVD (Physical vapor Deposition) processes as magnetron sputtering [2, 3], vacuum-arc deposition [4, 5], and hybrid methods [2, 4, 5–8], including a simultaneous use of ion sources, magnetrons, electric-arc evaporators, laser ablation systems, CVD (Chemical Vapor Deposition) apparatus and other facilities.

Currently, vacuum ion-plasma processes are thought to be the most promising methods of deposition of different types of (protective, hardening, wear-resistant, etc.) coatings; in this list the reactive magnetron sputtering and vacuum-arc deposition are being used quite extensively [2, 3, 9]. The main advantage of the magnetron method is droplet-free coating deposition [2, 3, 10]. Its critical limitations are: relatively high operating pressure supporting the discharge, narrow range of principal parameters (pressure and current) at which optimal coating-deposition conditions

[1]Institute of High-Current Electronics of the Siberian Branch of the Russian Academy of Sciences, Tomsk, Russia, e-mail: yufi55@mail.ru; shugurov@opee.hcei.tsc.ru; [2]National Research Tomsk State University, Tomsk, Russia, e-mail: krysina_82@mail.ru; elizmarkova@yahoo.com; [3]National Research Tomsk Polytechnic University, Tomsk, Russia, e-mail: ole.ts@mail.ru; [4]Tomsk State Architecture and Building University, Tomsk, Russia, e-mail: ivaov@mail.ru; Translated from Izvestiya Vysshikh Uchebnykh Zavedenii, Fizika, No. 5, pp. 118–125, May, 2017. Original article submitted January 16, 2017.

are realized, and low energy of the particles participating in the reactive synthesis of nitrides, which gives rise to large porosity of the resulting coatings and their relatively low adhesion to the substrates.

Using the vacuum-arc process of coating deposition based on the generation of highly ionized metal plasma by an arc discharge [4, 8], coatings are formed as a result of condensation of the flow of the eroding cathode material plasma on the specimen surfaces. The vacuum-arc deposition is generally carried out as a multistage process in a single vacuum cycle. In the first stage, the specimen surface is cleaned, heated and activated by inert gas ions, metal-containing ions, or reactive working gas ions. In the second stage, an auxiliary sublayer of varying elemental composition can be deposited in order to increase adhesion of the main coating to the substrate. In the third stage, the main coating is synthesized. The final stage assumes cooling of the modified specimens under the operating-vacuum conditions [11, 12].

In the case of the plasma-assisted vacuum-arc deposition performed in a hot-cathode plasma source (PINK) [13], low-pressure plasma of a nonsustained arc discharge is used in the first stage (surface cleaning, heating, and activation). In the course of gas-discharge plasma generation at low operating pressures (0.01–0.1 Pa), the mean ion free path increases and exceeds the characteristic size of the spatial charge layer formed near the substrate, to which a negative bias voltage is applied. When the value of the latter is varied, the ions hitting the substrate surface after propagating through the spatial charge layer formed near the substrate at low pressures are accelerated to the energy comparable with the applied potential, since the energy loss due to collisions with the other particles could be neglected. Thus using ions of the working gas (inert or reactive) with the energies within the interval 100–1000 eV, we can effectively clean the surface by etching the specimen surfaces (removing oxide films and adsorbed gases), heat them and activate for further ion-plasma processing (nitriding and coating deposition). It is expected that the multistage character of the vacuum-arc coating-deposition processes in a single vacuum cycle would result in the formation of gradient structural-phase states of the substrate material surface layer.

Today the most common coatings are those made from titanium nitride due to its excellent physical-mechanical, thermal-physical, anti-corrosive, and other characteristics and also its relative cheapness and ecological safety both in the deposition and application. The binary TiN system is frequently used as a wear resistant coating. It has a golden color and its hardness can vary from 20 to 54 GPa depending on the deposition parameters [4]. The coating can contain Ti_2N-phases with a tetragonal lattice and TiN-phases with a face-centered (FCC) lattice. The region of homogeneity of the Ti_2N-phase is extremely narrow; it is formed in a narrow range of nitrogen pressures (about 0.01 Pa). For this reason, the coating within this pressure range simultaneously contains a mixture of Ti_2N-phases with α-Ti or TiN and possesses maximum porosity. Such coatings are however practically unserviceable due to their high brittleness. The TiN_x compound [8] forms a $B1$ crystal lattice (NaCl-type structure) representing two cubic lattices of titanium and nitrogen embedded in each other. The degree of stoichiometry x varies within the range from 0.6 to 1.2; at $x < 1$ the nitrogen sublattice is defective, having vacancies in the nitrogen positions [5]. According to the data reported in [4], the TiN lattice parameter varies within a = 0.425–0.426 nm in a wide rage nonstoichiometry (x = 0.9–1.5). As the nitrogen pressure increases up to 1 Pa, microhardness of the coatings decreases and they become single-phased (TiN) and more resistant to wear during cutting and erosion [14]; the content and size of the droplet fraction also decreases. Nonstoichiometric, single-phased coatings, such as TiN with the microhardness about 25 GPa are resistant to different types of wear; the content of nitrogen in them is nearly 40% [15].

The purpose of this work is to analyze the phase composition and defect structure of the surface layer of technical-grade titanium formed in the course of the vacuum-arc, plasma-assisted deposition of titanium nitride coatings carried out using a hot-cathode plasma source.

MATERIAL AND EXPERIMENTAL PROCEDURES

The material was VT1-0 technically pure titanium (Al–0.7, Fe–0.25, Si–0.10, C–0.07, N–0.04, 0.20 H–0.010 Ni, 0.10 Cu, 0.08 Ni, 0.01(Cr+Mn), rest Ti, wt.%) [16]. The specimens were 5 mm thick plates measuring 15×15 mm. The deposition of TiN thin (0.5 μm) films on the substrates made from VT1-0 technical-grade titanium was performed in a novel, automated vacuum ion-plasma facility QUINTA [17]. Before deposition of the coating, the specimens were mechanically polished to Ra = 0.02 μm. The specimens were fixed on the substrate placed at a distance of 320 mm from

the output aperture of the arc evaporator. In the course of a large number of experiments, we identified an optimal scheme of coating synthesis, specifically: cleaning in the argon plasma generated by a PINK plasma source (I_{PINK} = 20 A, U_{bias} = 900 V) at the working gas pressure in the chamber 0.17 Pa within 15 min; surface heating and activation using titanium plasma generated by the arc evaporator (arc current I_{arc} = 80 A, substrate bias voltage U_{bias} = 900 V, dwell time 30 s, working chamber gas pressure 0.17 Pa); formation of a titanium sublayer via evaporation of the cathode made from VT1-0 technical-grade titanium (arc current I_{arc} = 80 A, substrate bias voltage U_{bias} = 50 V, dwell time 30 s, working chamber gas pressure 0.17 Pa); specimen heating to 350°C (specimen temperature during deposition) by ion bombardment; replacement of argon by nitrogen and coating deposition during 3 min 30 s at the optimal parameters (nitrogen plasma generator current 20 A; arc evaporator current (titanium plasma formation) 80 A; substrate bias voltage U_{bias} = 150 V; nitrogen pressure in the working chamber 0.3 Pa). After their deposition the coatings were cooled in vacuum for 1 hour.

The phase composition of the coating (TiN)/substrate (VT1-0) system was examined by the methods of X-ray diffraction analysis (XRD 6000 diffractometer; X-ray exposure in a tangent geometry (incident angle 1°)). The material defect structure was analyzed by the methods of diffraction electron microscopy (method of thin foils) (JEM-2100 F microscope). The foils measuring 150–250 nm in thickness were cut for electron microscopy using spark cutting from a monolithic workpiece perpendicular to the surface of modification and thinned by ion-beam sputtering. The hardness and Young's modulus of the surface layer of the coating (TiN)/substrate (VT1-0) system were determined at normal indenter loads varied within the interval from 10 to 300 mN (Nano Hardness Tester NHT-S-AX-000X).

EXPERIMENTAL RESULTS AND DISCUSSION

Using the methods of X-ray diffraction analysis it has been found that the formation of the coating (TiN)/substrate (VT1-0) system is accompanied, in addition to the formation of TiN, by the substrate modification, which is observed as deformation of the crystal lattice of α-titanium (decreased parameter *a*, increased parameters *c* and hence *c*/*a*, and increased microdistortions). It could be assumed that the reason for these results is the saturation of the crystal lattice of α-titanium with nitrogen atoms.

The crystal lattice parameter of the titanium nitride TiN formed in the coating is found to be 0.42584 nm, which, according to the data reported in [4], corresponds to the level of stoichiometry x = 0.9–1.5.

The resulting modified layer is comparatively thin, which is indicated by the nanoindentation data. The hardness, a factor of 1.6 higher than that of α-titanium, is observed at the indenter loads smaller than 50 mN only; high values of the Young's modulus (≈200 GPa), which are indicative of the formation of the nitride coating, are revealed at the indenter load 10 mN only. Note that thicker (3–5 μm and more) coatings of the TiN composition are characterized by the hardness varying from 20 to 54 GPa and the Young's modulus within 500–640 GPa, whose value depends on the content of nitrogen in the coating [18, 19]; according to other data this value lies in the range 384–446 GPa and depends on the substrate material [20].

The defect structure and phase composition of the coating (TiN)/substrate (VT1-0) system were analyzed by the methods of diffraction electron microscopy of thin foils. A characteristic image of the ≈ 8 μm surface layer structure is presented in Fig. 1*a*.

It is clearly seen that during the coating formation process a multilayer, highly defective structure is formed. As the distance from the modified surface increases, the level of defects decreases (Fig. 1*b*, the layer at the depth 15–25 μm) and at the depth 35–40 μm a structure similar to that of the initial titanium is observed, specifically, these are the grains containing a dislocation chaos substructure in the bulk; the scalar dislocation density is $\approx 0.6 \cdot 10^9$ cm^{-2} (Fig. 1*c*).

Figures 2–4 depict the structure of the modified layer ≈2 μm in thickness in greater detail. Shown in Fig. 2 is the electron microscopy image of the surface layer structure (Layer 1 in Fig. 1*a*), whose thickness varies from 300 to 350 nm. The alloy in question has polycrystalline structure. The sizes of the crystallites possessing quasi-equiaxed shape vary within the range from 20 to 50 nm. In their bulk and at the boundaries of these crystallites there are inclusions whose dimensions vary within 2–5 nm. Thus the surface layer formed as a result of vacuum-arc, plasma-assisted deposition could be classified as nanocrystalline in terms of its grain size. The phase composition of this layer was determined by indexing the microelectron diffraction patterns (microED patterns) obtained from its surface.

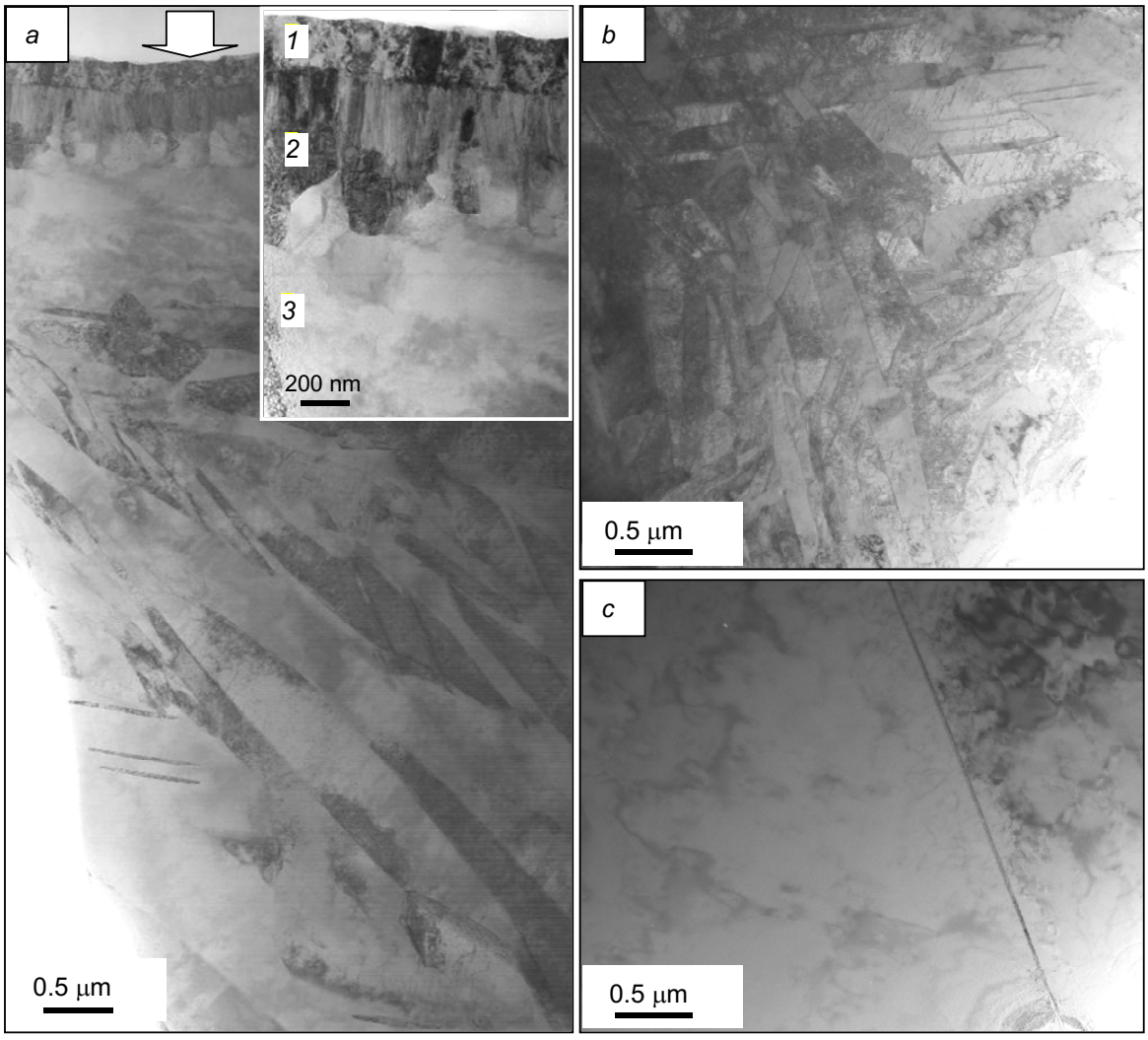

Fig. 1. Electronic image of the structure forming in the surface layer of VT1-0 technically pure titanium during deposition of a thin TiN coating: surface layer structure (*a*), material structure at the depth 15–25 μm (*b*), at the depth 35– 45 μm (*c*). The arrow in (*a*) indicates the modified surface.

In Fig. 2, the area from which this microED pattern was obtained is circumscribed. An analysis of the microED pattern made it possible to identify the reflections belonging to crystal lattice of titanium nitrides, TiN and Ti_2N. Based on their relative intensity, we can draw a conclusion that the major phase of the surface layer is TiN. We might assume Ti_2N to be located along the grain boundaries and in the bulk of TiN in the form of aforementioned inclusions measuring 2–5 nm. A dark-field image of the surface layer structure, obtained in the [002] TiN reflection, demonstrates that the grains of titanium nitride are broken into weakly misoriented areas measuring 4–6 nm, which corresponds to the dimensions of coherently diffracting domains identified by the methods of X-ray diffraction analysis (Table 1).

The surface layer structure (Layer 2 in Fig. 1*a*) is presented in Fig. 3. An analysis of the bright- and dark-field images from this layer allows us to divide it into two sublayers (Fig. 3). The sublayer adjacent to the surface layer has columnar structure. The columns are oriented perpendicular to the surface of modification. The lateral dimensions of the columns vary within 50–80 nm. The columns are broken into weakly misoriented layers 10–15 nm in thickness. It should be noted that the TiN ion-plasma coatings generally possess columnar structure with thread-like grains 25–70 nm in diameter, elongated towards the growth direction. The average diameter of the columns is ≈200 nm [21, 22].

TABLE 1. XRD Data from Technical-Grade Titanium and the Coating (TiN)/Substrate (VT1-0) System

Material	Phase	Lattice parameter, nm		*C*/*A*	Δ*V*,%	Δ*d*/*d* ·10^3	*D*(CDDs), nm
		a	*c*				
BT1-0 initial	α-Ti	0.29485	0.46778	1.5865	100	1.5	14
BT1-0+TiN	α-Ti	0.29464	0.46836	1.590	52.4	2	15
	TiN	0.42584			47.6	4.7	10

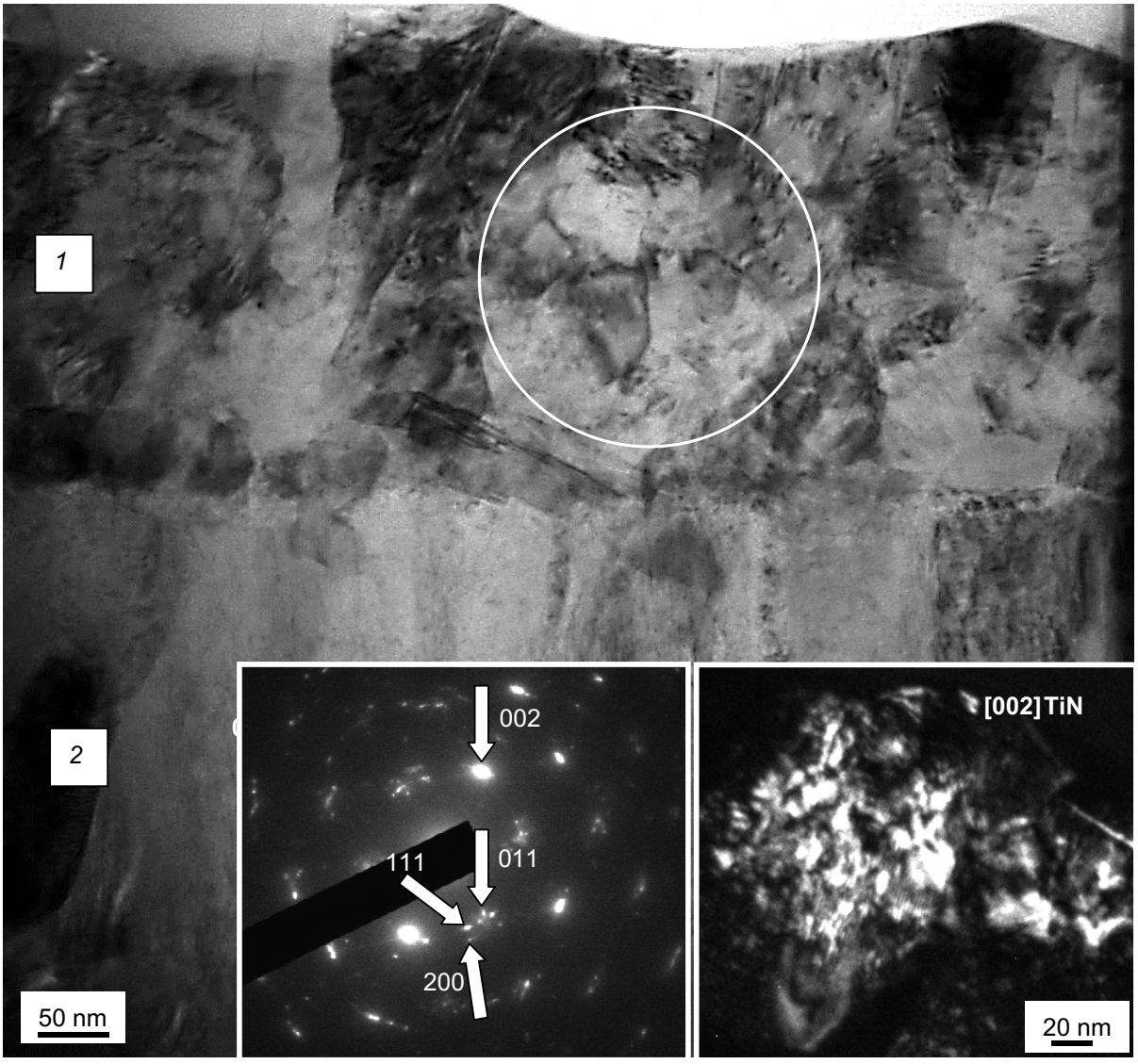

Fig. 2. Electron-microscope image of the surface layer structure (Layer 1 in Fig. 1) of the coating (TiN)/substrate (VT1-0) system; the dark field image obtained in the [002]TiN reflection (indicated by an arrow). The microED pattern features the [111]TiN, [200]TiN and [011]Ti_2N reflections; the area of the foil from which this pattern was obtained is circumscribed.

The sublayer adjacent to the specimen bulk is formed by quasi-axial crystallites, which is clearly seen in the dark-field image of the structure. The crystallites size varies within the range 50– 280 nm.

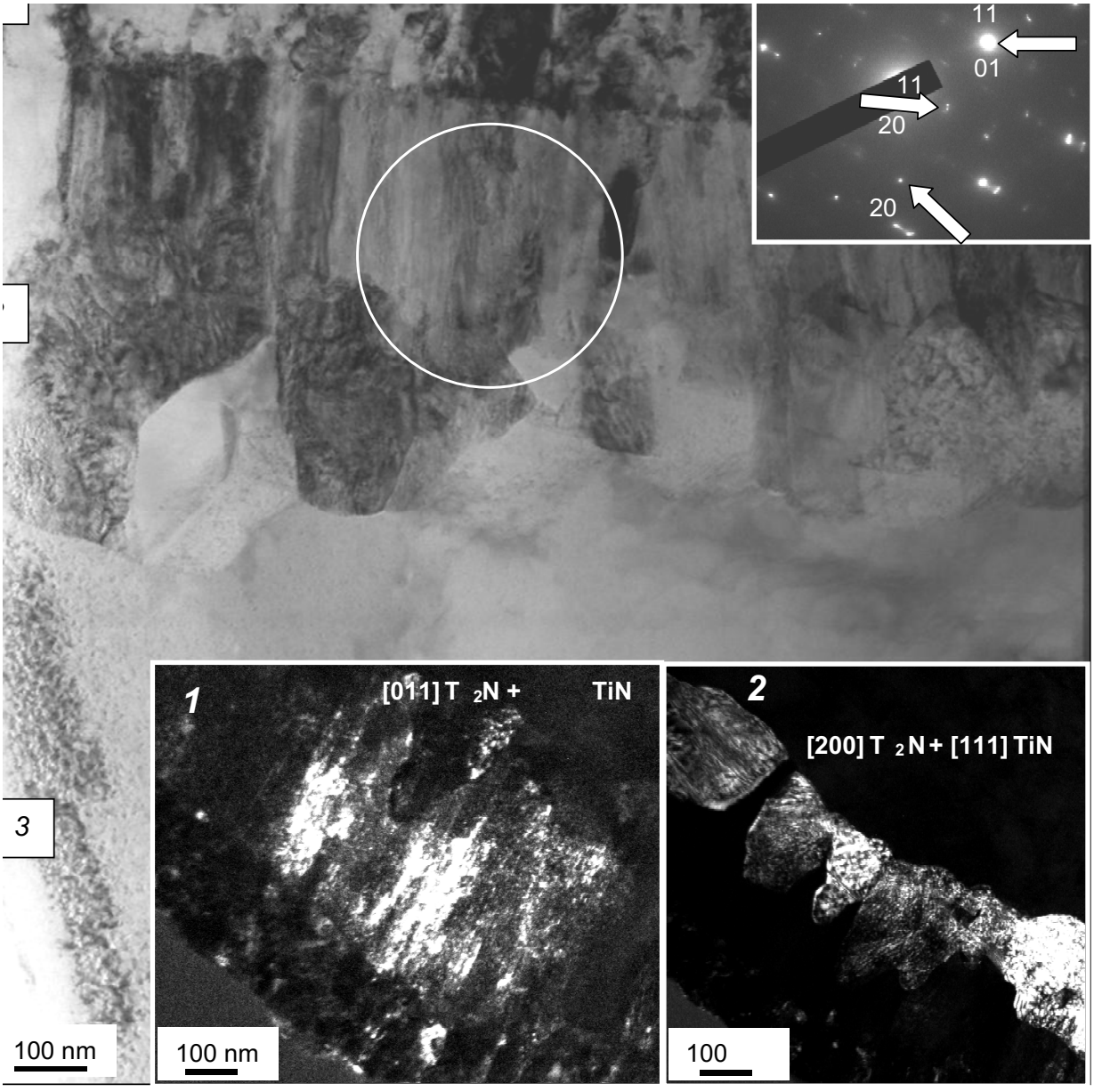

Fig. 3. Electron-microscope image of the surface layer structure (Layer 2) of the coating (TiN)/substrate (VT1-0) system; the dark field images were obtained in the following reflections (indicated by the arrows in the microED pattern): [011]Ti_2N + [111]TiN (*1)*, [200]Ti_2N + [111]TiN (*2*). The area of the foil from which this pattern was obtained is circumscribed.

An indexing of the microED pattern obtained from this layer (from an area circumscribed in Fig. 3) revealed the presence of reflections belonging to the crystal lattices of titanium nitrides, TiN and Ti_2N. Based on the relative intensity of the reflections from the crystal lattices of these phases, one can draw a conclusion that the major phase of the transition layer is the Ti_2N titanium nitride.

An electron-microscopy image of the structure of Layer 3 is presented in Fig. 4. The major phase of this layer, as shown by the indexing of the respective microED pattern, is α-titanium. The second phase of this layer is titanium

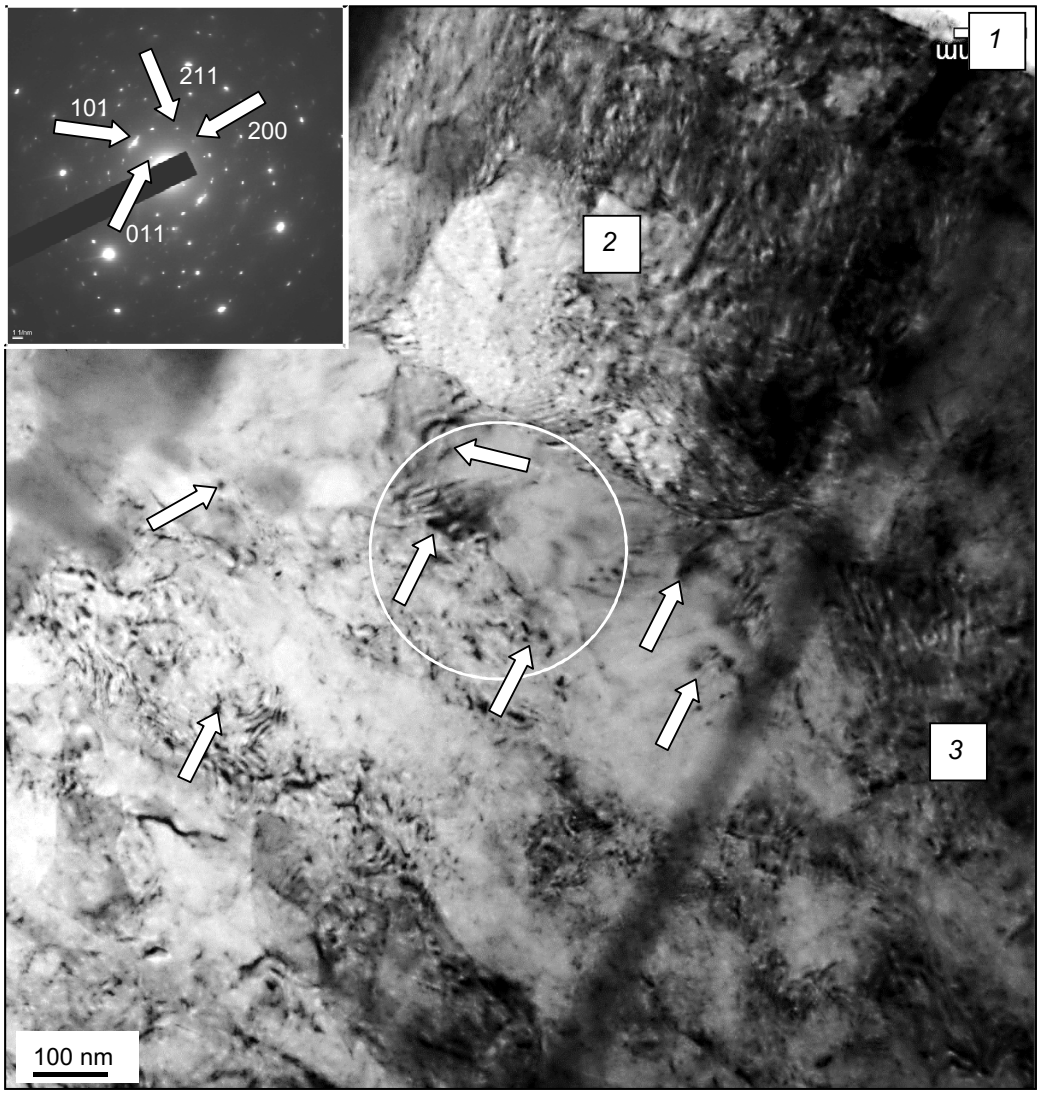

Fig. 4. Electron-microscope image of the surface layer structure (Layer 3) of the coating (TiN)/substrate (VT1-0) system. The microED pattern features the [101]α-Ti, [200]Ti_3N, [011]Ti_3N and [211]Ti_3N reflections. The area of the foil from which this pattern was obtained is circumscribed. The arrows in the bright-field image of the α-Ti structure indicate Ti_3N-precipitates.

subnitride of the Ti_3N composition, whose presence was reported in [23]. The particles of titanium subnitride have round shapes and their sizes lie within 3–6 nm.

SUMMARY

An analysis has been performed of the phase composition and defect substructure of the surface layer of technical-grade titanium formed during vacuum-arc, plasma-assisted deposition of a titanium nitride coating using a hot-cathode plasma source (PINK). Before the deposition the following processing was carried out: cleaning of the specimen surface in argon plasma generated by a PINK plasma source, its heating and activation using titanium plasma

generated by an arc evaporator; deposition of a titanium sublayer by evaporating a VT1-0 technical grade titanium cathode, and heating of the specimens by ion bombardment to 350 °C (the specimen temperature during coating deposition). The formation of multilayer, multiphase structure has been observed, whose thickness is up to 40 μm. It has been demonstrated that the surface layer, whose thickness varies within the range from 20 to 50 nm, possesses polycrystalline structure. The major phase of the surface layer is titanium nitride of the TiN composition; the second phase is titanium nitride of the Ti_2N composition with the particle sizes 2–5 nm. The transition layer, based on its morphology, can be divided into two sublayers. The sublayer adjacent to the surface layer has columnar structure, with the column dimensions varying in the range 50–80 nm. The columns are divided into weakly misoriented layers 10–15 nm in thickness. The sublayer adjacent to the specimen bulk consists of quasi-axial crystallites, whose dimensions vary within 150–280 nm. The major phase of the transition layer is titanium nitride of the TiN composition. The volume of α-titanium adjacent to the transition layer contains round-shape inclusions of titanium subnitride; the particles measure 3–6 nm. It is expected that the principal reason for formation of the multilayer, multiphase structure during deposition of nitride coatings onto the specimens of VT1-0 technical-grade titanium is a multistage character of the process of material modification carried out in a QUINTA facility under conditions of common vacuum.

This study has been partially funded by an RFBR grant (Project No. 16-58-00075).

REFERENCES

1. A. A. Ilyin, B. A. Kolachev, and I. S. Polkin, Titanium Alloys. Composition, Structure, Properties: reference book [in Russian], VILS-MATI, Moscow (2009).
2. E. V. Berlin and L. A. Seidman, Ion-Plasma Processes in Thin-Film Technology [in Russian], Tekhnosfera, Moscow (2010).
3. A. I. Kuzmichev, Magnetron Sputtering Systems [in Russian], Avers, Kiev (2008).
4. A. A. Andreev, L. P. Sablev, V. M. Shulaev, and S. N. Grigoriev, Vacuum-Arc Facilities and Coatings [in Russian], NNC HFTI, Kharkov (2005).
5. A. A. Andreev, L. P. Sablev, and S. N. Grigoriev, Vacuum-Arc Coatings [in Russian], NNC HFTI, Kharkov (2010).
6. Hyun S. Myung, Hyuk M.Lee, Leonid R. Shaginyan, and Jeon G. Han, Surf. Coatings Technol., **163-164**, 591–596 (2003).
7. Hyun S. Myung , Jeon G. Han , and Jin H. Boo, Surf. Coatings Technol., **177-178**, 404–408 (2004).
8. V. A. Barvinok and V. I. Bogdanovich, Principal Physics and Mathematical Modeling of the Processes of Vacuum- Ion-Plasma Deposition [in Russian], Mashinostroyeniye, Moscow (1999).
9. E. V. Berkin, N. N. Koval, and L. A. Seidman, Plasma-Assisted Chemical-Thermal Processing of Steel Components [in Russian], Tekhnosfera, Moscow (2012).
10. E. V. Berkin, S. A. Dvinin, and L. A. Seidman, Vacuum Technology and Equipment for Deposition and Etching of Thin Films [in Russian], Tekhnosfera, Moscow (2007).
11. Electron-Ion-Plasma Modification of Nonferrous Metals and Alloys (Eds. N. N. Koval and Yu. F. Ivanov) [in Russian], NTL Publ., Tomsk (2016).
12. Surface Layer Structure Evolution in Steel Subjected to Electron-Ion-Plasma Treatment (Eds. N. N. Koval and Yu. F. Ivanov) [in Russian], NTL Publ., Tomsk (2016).
13. L. G. Vintizenko, S. V. Grigoriev, N. N. Koval, *et al*., Russ. Phys. J., **44**, No. 9, 927–936 (2001).
14. T. Ikeda and H. Satoh, Thin Solid Films, **195**, 99–110 (1991).
15. J. A. Sue, Surf. Coatings Technol., **61**, 115–120 (1993).
16. E. A. Borisova, G. A.Bochvar, M. Ya. Brun, *et al*., Titanium Alloys. Metallography of Titanium Alloys [in Russian], Metallurgiya, Moscow (1980).

17. N. N. Koval, Yu. F. Ivanov, I. V. Lopatin, *et al*., Ross. Khim. Zh. (J. of the D. I. Mendeleyev Russian Chemical Siciety), **LVII**, Nos. 3–4, 121–133 (2013).
18. S. Luridiana and A. Miotello, Thin Solid Films, **290–291**, 289–293, (1996).
19. E. Torok, J. Perry, L. Chollet, and W.-D. Sproul, Thin Solid Films, **153**, 37– 43 (1987).
20. J. R. Roos, J. P. Selis, E. Vancoille, *et al*., Thin Solid Films, **193/194**, 547–556 (1990).
21. L. A. Dobrzanski and M. Adamiak, J. Mater. Proc. Technol., **133**, 50–62 (2003).
22. R. L. Boxman, V. N. Zhitomirsky, I. Grinberg, *et al*., Surf. Coatings Technol., **125**, 257–262 (2000).
23. G. P. Luchinskii, Chemistry of Titanium, Khimiya, Moscow (1971).